Mon. Not. R. astr. Soc. (1972) **160**, 99–119.

DIELECTRONIC SATELLITE SPECTRA FOR HIGHLY-CHARGED HELIUM-LIKE ION LINES

A. H. Gabriel

(Received 1972 June 5)

SUMMARY

Calculations have been carried out in intermediate coupling of the wavelengths and intensities of the satellite lines situated on the long wavelength side of the helium-like ion resonance lines, recently observed from solar flares. Earlier calculations up to aluminium have been extended up to iron and copper. For the intensities, the important processes are primarily dielectronic recombination, but also direct inner-shell excitation. Comparisons have been made with spectra from solar flares and active regions, and from low-inductance laboratory sparks. Computed wavelengths in iron are found to agree with these to better than 0·0003 Å. Comparison of the intensities allows the determination of both the electron temperature and the transient ionizing state of the plasma. The laboratory plasma spectra are found to be in an extreme transient ionizing condition, and are thus significantly different from solar spectra. In the cases studied, solar active regions were found to be moderately ionizing, while the flare spectra were recombining.

1. INTRODUCTION

Satellite lines situated on the long-wavelength side of helium-like resonance lines were first reported from laboratory spark sources by Edlén & Tyrén (1939), who assigned configurations

$$1s^2nl - 1s2pnl.$$

Gabriel & Jordan (1969a) classified the terms responsible by comparing computed spectra with observations, over the range carbon IV to aluminium XI. They also proposed that the dominant mechanism for production of these states is by dielectronic recombination. A theory for the intensity of the satellites was first derived by Gabriel, Jordan & Paget (1969) and expressed in more detail by Gabriel & Paget (1972), hereafter referred to as Paper I. In Paper I, observations on a laboratory plasma in oxygen and nitrogen were compared with intensities derived from theory.

Calculation of the wavelengths of the satellites can be carried out in an LS approximation up to aluminium. Theory for the intensities also has a simple low Z approximation, valid in this case as far as neon. However, recent observations of the soft X-ray emission from solar active regions and flares has recorded such satellites to helium-like ions as far as iron XXV. The present work aims to extend the calculations, both for wavelengths and intensities, up to these higher ions. Since the intensity of the satellites relative to the resonance line is a function of electron temperature this then leads to a method for the measurement of temperature in solar flares. Although *ab initio* methods are used for the calculations, use is made of reliable observations in carbon, oxygen and magnesium in order to adjust

empirically the computed wavelengths. In this way it is hoped that the most reliable predictions can be made for the higher Z ions, where observational data is at present rather scarce.

In Paper I, two mechanisms were considered for the population of the initial states of the satellite transitions; dielectronic recombination from the helium-like ion, and inner-shell excitation of the lithium-like ion. It was shown that for low Z ions, the second process is negligible except in conditions of transient ionization. For the higher Z ions considered here, inner-shell excitation makes a relatively greater contribution, although even for iron, the dominant mechanism in the steady state is still dielectronic recombination. However, solar flares might be expected to depart somewhat from steady state ionization. The present paper therefore makes an attempt to include the effects of inner-shell excitation, although the probable accuracy for this contribution is perhaps only a factor of ~ 2.

In addition to the satellite lines, the same wavelength region also contains the intercombination and forbidden lines of the helium-like ion. Interpretation of an observed spectrum therefore requires in addition a knowledge of the accurate wavelengths and predicted intensities of these features.

2. THEORY

2.1 *Dielectronic recombination*

The mechanism of formation of the satellites by dielectronic recombination has been discussed in detail in Paper I. The satellite intensity, in photons per unit volume is given by

$$I_s = N_{He} N_e \frac{4\pi^{3/2} a_0^3}{T^{3/2}} \frac{g_s}{g_1} A_r \frac{A_a}{(A_a + \sum A_r)} \exp(-E_s/T) \qquad (1)$$

where N_{He} and N_e are the density of helium-like ions and electrons; g_s and g_1 are statistical weights of the satellite level and the helium-like ground state; A_a and A_r are transition probabilities for decay by autoionization and radiation, and the summation is over all possible radiative transitions from the satellite level. E_s is the energy of the satellite level above the helium-like ground state, and T is the electron temperature, both in atomic units of 1 Rydberg.

The intensity of the helium-like ion resonance line is given by

$$I = N_{He} N_e C(1 + \alpha) \qquad (2)$$

where C is the impact excitation rate coefficient. α is a correction for the contribution to the resonance line intensity from dielectronic recombination, i.e. it is the sum over all satellites which cannot be resolved spectroscopically from the resonance line. For this work it will be taken to include $n \geqslant 3$. We can then write

$$\alpha = D/C \qquad (3)$$

where D is that fraction of the dielectronic recombination rate coefficient responsible for this contribution.

Following Van Regemorter (1962), C can be written

$$C = 8 \sqrt{\frac{\pi}{3}} \frac{h a_0}{m} \frac{f}{E_0 T^{1/2}} P \exp(-E_0/T) \qquad (4)$$

where E_0 is the energy of the resonance line, P an effective Gaunt Factor of 0·2,

and f the oscillator strength. Here this approximate formula is adjusted semi-empirically by regarding $\bar{f}$ as an adjustable parameter. It was shown in Paper I that experimentally $\bar{f} \sim 0{\cdot}75$ for excitation to $1s2p\,^1P$ plus $1s2s\,^1S$. At the lower densities relevant to astrophysics, $1s2s\,^1S$ will decay by two-photon emission, rather than by transfer to $1s2p\,^1P$, and we then adopt $\bar{f} = 0{\cdot}55$ for excitation to the $1s2p\,^1P$ term alone. The critical density N_e'' for the transition between these two conditions is given by

$$N_e'' \sim \frac{A(1s2s\,^1S \rightarrow 1s^2\,^1S)}{C(1s2s\,^1S \rightarrow 1s2p\,^1P)} \tag{5}$$

which we can write approximately as

$$N_e'' \sim 7.10^5(Z-1)^{9{\cdot}3}\ \mathrm{cm}^{-3} \tag{6}$$

where Z is the *nuclear* charge of the ion. To avoid confusion, this definition of Z will be used throughout this paper.

Combining equations (1), (2) and (4) in numerical form, taking $\bar{f} = 0{\cdot}55$, and noting that $g_1 = 1$, the ratio of a satellite to the resonance line intensity becomes

$$\frac{I_s}{I} = \underbrace{\frac{0{\cdot}01104}{(1+\alpha)}\frac{E_0}{T}\exp\left[(E_0-E_s)/kT\right]}_{\frac{1}{(1+\alpha)}F_1(T)} \times \underbrace{\frac{g_s A_r A_a}{(A_a+\sum A_r)}}_{F_2(S)} \tag{7}$$

where T is now in °K, and E_0 and E_s in eV. The intensity ratio can thus be separated into a function of electron temperature, $F_1(T)/(1+\alpha)$, and a function of the individual satellite line $F_2(S)$.

In order to derive α we use Burgess's (1965) semi-empirical formula for the dielectronic recombination coefficient, slightly modified as follows:

$$R = \frac{4{\cdot}8\times 10^{-11}}{T^{3/2}}\frac{(Z-2)^{1/2}(Z-1)^2}{(Z^2-2Z+17{\cdot}4)^{1/2}} f E_0^{1/2}\frac{1}{(1+0{\cdot}105x+0{\cdot}015x^2)}\exp(-E_0/T) \tag{8}$$

Here, T and E_0 are in Rydbergs and x is given by $E_0/(Z-1)$. Z is the nuclear charge as before. Only one term in Burgess's summation appears in equation (8) since we are concerned only with satellites to the one resonance line. It is clear that R in equation (8) includes both the unresolved and resolved satellites. In Paper I for ions of $Z = 7$ and 8, the latter were assumed to make a negligible contribution and D was put equal to R, or $\alpha = R/C$. However for higher Z, the resolved satellites make an increasingly significant contribution to R and a correction must be applied. Shore (1969) has pointed out that Burgess's theory is a bad approximation for low n. In particular, it assumes that the $1s2pnl$ state has a statistical weight of $12\times 2n^2$, whereas for $n = 2$ not all of this is available due to the exclusion principle, and in fact only a weight of 24 is autoionizing in LS coupling (compared with 72 in Burgess's approximation). Also equation (8) assumes $E_0 = E_s$ which is bad for $n = 2$. We therefore make the approximate correction

$$\alpha = \frac{R}{C} - \exp\left[-(E_0-E_s)/T\right]\times 3\times F_1(T)\sum_{n=2} F_2(S), \tag{9}$$

where the exponential term and the factor of 3 are introduced to allow for the above-mentioned effects. The second term becomes equal to the first for ions above silicon. This is partly due to errors in the approximations used, but emphasizes that for higher helium-like ions dielectronic recombination takes place primarily through the $n = 2$ satellite levels. The value of α used thus rises slowly to a maximum of $\sim 0{\cdot}1$ for fluorine and then drops to zero for silicon and above. For this 10 per cent correction term, the above approximations are considered adequate.

The above theory for the intensity of the satellites is carried out in a scheme in which the satellite level and the adjacent continuum are considered as separate states. This is not strictly correct, since the autoionizing satellite levels are not true stationary states. However, it is a legitimate approximation as pointed out by Shore (1969). Neglecting the interacting continuum, when calculating the energy of the satellite levels, introduces an error which is of the order of the autoionizing widths of the levels. This error is negligible compared with other approximations in the computation.

2.2 *Inner-shell excitation*

The intensity I_s' of a satellite line produced by inner-shell excitation of the lithium-like ion can be written (see Paper I)

$$I_s' = N_{\mathrm{Li}} N_e C' \frac{A_r}{(A_a + \sum A_r)}. \tag{10}$$

The collision rate C' must be known, and in this paper we use the approximate form of equation (4) with the effective oscillator strength $\bar{f}'$ as an adjustable parameter. In particular, we assume that simultaneous excitation of two electrons is improbable and is thus neglected. Thus the configuration $1s2p^2$ is excited only from the excited state $1s^2 2p$. The configuration $1s2s2p$ can be excited from either $1s^2 2s$ or $1s^2 2p$, but only the first is considered as it is expected to dominate. Equation (10) can then be rewritten

$$I_s' = N_{\mathrm{Li}} N_e C' \beta \frac{A_r}{(A_a + \sum A_r)}, \tag{11}$$

where β is the proportion of N_{Li} that is in the appropriate lower state, depending on which satellite is considered.

At low densities most of the population of the lithium-like ion is in its ground state. β is then 1 for the $1s2s2p$ configuration and zero for $1s2p^2$. At densities above some critical density N_e' a Boltzmann distribution is set up between $1s^2 2s$ and $1s^2 2p$. Then we get $\beta = \frac{1}{4}$ for the $1s2s2p$ configuration and $\beta = \frac{3}{4}$ for the $1s2p^2$ configuration. The value of N_e' can be obtained from

$$N_e' \sim \frac{A(1s^2 2p^2 P \rightarrow 1s^2 2s^2 S)}{C(1s^2 2s^2 S \rightarrow 1s^2 2p^2 P)}. \tag{12}$$

This can be rewritten approximately as

$$N_e' \sim 6.10^{12}(Z-2)^{4\cdot 3}\ \mathrm{cm}^{-3}. \tag{13}$$

If we express the inner-shell contribution to the satellite as a proportion of the resonance line intensity, we get from (2) and (11)

$$\frac{I_s'}{I} = \frac{N_{\mathrm{Li}}}{N_{\mathrm{He}}} \frac{C'}{C} \frac{A_r}{(A_a + \sum A_r)} \frac{\beta}{(1+\alpha)}. \tag{14}$$

Since the energies involved in C' and C are approximately equal the ratio of C's reduces to the ratio of the effective oscillator strengths $\bar{f}$.

The ion abundance ratio $N_{\mathrm{Li}}/N_{\mathrm{He}}$ is a function both of the electron temperature T and of the departure from ionization equilibrium. We define an ionization temperature T_z which is the temperature at which the actual ratio $N_{\mathrm{Li}}/N_{\mathrm{He}}$ would exist in ionization equilibrium. Then $N_{\mathrm{Li}}/N_{\mathrm{He}}$ is a function only of T_z; also $T_z = T$ for ionization equilibrium, $T_z < T$ for transient ionizing conditions and $T_z > T$ for transient recombining conditions. Then equation (14) can be divided into temperature dependent and satellite dependent terms:

$$\frac{I_s'}{I} = \underbrace{\frac{N_{\mathrm{Li}}}{N_{\mathrm{He}}}\frac{1}{(1+\alpha)}}\times\beta\underbrace{\frac{\bar{f}'}{\bar{f}}\frac{A_r}{(A_a+\sum A_r)}}. \qquad (15)$$

$$= \frac{1}{(1+\alpha)}F_1'(T_z)\times \qquad \beta F_2'(S)$$

The problem reduces to choosing the appropriate values for $\bar{f}'$ the effective oscillator strength for the excitation. In this, one is guided by the similarity between these excitations and those in helium-like ions, and can draw on the experimental and theoretical evidence available for those ions. The values used are listed in Table I. For those transitions allowed in LS coupling, the $\bar{f}'$ used was the actual oscillator strength computed in the present work. The others have been scaled from these,

TABLE I

Effective oscillator strengths $\bar{f}'$, for inner-shell excitation rate coefficients

$1s^2 2p\,^2P^0 \rightarrow 1s2p^2\,^2P$	Computed
^4P	$\frac{1}{2}\times\bar{f}(^2P^0\text{–}^2P)$
^2D	Computed
^2S	Computed
$\rightarrow 1s2s^2\,^2S$	$\frac{1}{3}\times\bar{f}(^2P^0\text{–}^2S)$
$1s^2 2s\,^2S \rightarrow 1s2p(^1P)2s\,^2P^0$	Computed
$\rightarrow 1s2p(^3P)2s\,^2P^0$	$\frac{1}{3}\times\bar{f}(^2S\text{–}(^1P)\,^2P^0)$
$^4P^0$	$\frac{1}{3}\times\bar{f}(^2S\text{–}(^1P)\,^2P^0)$

as shown in Table I. The excitation rate was then divided amongst the fine structure levels of each term according to their statistical weights.

3. COMPUTATIONAL METHOD

3.1 *Energies*

The method used for calculating the satellite energies is an extension of that used by Gabriel & Jordan (1969a) for the lower Z ions, carbon to aluminium. In that work, Hartree–Fock calculations were carried out for the initial and final levels of the transitions in LS coupling. Similar calculations were made for the helium-like ion resonance line and the comparison with observations was made using the *difference* between the transition energies of the satellites and the helium-like ion resonance line. This ' double difference ' method helped to eliminate many of the systematic errors inherent in the Hartree–Fock method. Even so, in this earlier work, there were residual errors between the computed and observed energies for

three of the stronger satellites. These errors can be represented as simple linear functions of Z, are not therefore due to the neglect of higher order relativistic terms.

For the present work, the technique used includes also the effect of spin-orbit interaction, i.e. it is a full intermediate coupling calculation, extended up as far as copper. Other relativistic terms are not included, since these tend to cancel in the ' double difference ' approach. Thus, the calculations give only the energy differences between the satellite transitions and the helium-like ion resonance line. Furthermore, the known satellite energies at low Z have been used to provide corrections, linear in Z, for those satellites for which discrepancies were found previously. The important steps in the calculation are as follows.

Calculations were carried out using the Froese (1969) Hartree–Fock method with configuration mixing, for a set of zero-order terms in LS coupling. These terms are listed in Table II. The configuration mixing facility was not used directly,

TABLE II

Zero-order terms used in the calculation

Satellite initial	$1s2p^2$	^4P
		^2P
		^2D
		^2S
	$1s2s^2$	^2S
	$1s2p(^3P)2s$	$^4P^0$
		$^2P^0$
	$1s2p(^1P)2s$	$^2P^0$
Satellite final	$1s^22p$	$^2P^0$
	$1s^22s$	^2S
He-like initial	$1s2p$	$^3P^0$
		$^1P^0$
	$1s2s$	^3S
He-like final	$1s^2$	^1S

but for the two pairs of bracketed terms, values were obtained for the zero-order energies (no mixing) and the off-diagonal electrostatic interaction. The calculation also gave the spin-orbit interaction energy for the $2p$ orbital. The computations were made for five elements; carbon, oxygen, silicon, calcium and iron. The computed energies were then interpolated and extrapolated from carbon to copper, using the appropriate asymptotic variation. The electrostatic energies were adjusted where necessary, as indicated above, to fit the observed satellite energies in carbon, oxygen and magnesium. Zero-order energy matrices were set up for each element for each LSJ level, using total electrostatic plus spin-orbit energies. The matrices were then diagonalized to give the full intermediate coupling energies, together with the eigenvectors of the transformation.

Cancellation of higher order relativistic corrections can only be relied upon when all the differences apply to the same single electron transition, i.e. $1s-2p$. We do not therefore expect the computed energies for the $1s^22p^2S-1s2s^22S$ and $1s^21S-1s2s^3S$ to be as accurate as the others. Since the second of these is an important intense line, more accurate calculations of its energy by Vainstein & Safronova (1971a) have been used in place of the present calculations. For the

remaining helium-like ion transitions, the present calculations have been used, and are in good agreement with the energies quoted by Vainstein and Safronova.

3.2 *Intensities*

Equations (7) and (15) show that for either mechanism the satellite intensities can be separated into a line factor and a temperature dependent term. The line factor depends on the quantities A_r and A_a. For the studies on nitrogen and oxygen carried out in Paper I, it was possible to simplify equation (7) since $A_a \gg A_r$. The factor $F_2(S)$ then becomes simply $g_S A_r$ and the satellite intensity is independent of A_a, which need not therefore be known. Since A_r varies as Z^4 whereas A_a is to a first order independent of Z, the above inequality breaks down for the heavier ions. Both A_a and A_r must then be known.

The choice of the zero-order terms in Table II was made in order to simplify the determination of A_r. Thus, in this scheme, the LS selection rules cause many of the transitions to vanish. In particular, all transitions from the quartet levels vanish, as does $1s^2 2s^2 S - 1s2p(^3P)2s^2P^0$ and $1s^2 2p^2 P^0 - 1s2s^2 {}^2S$. The allowed transitions can all be obtained from the radial dipole matrix element by the simple application of the usual multiplet strength factors. The radial dipole matrix element was computed using the radial wavefunctions obtained from the Hartree–Fock calculation. In this way, values of A_r were obtained for all transitions in the zero-order scheme. The transition probability $A_r(fi)$ between initial state i and final state f in intermediate coupling is then obtained from

$$A_r(fi) = \left[\sum_{a,b} V(a|i)\, V(b|f)\sqrt{A_r(ba)}\right]^2, \qquad (16)$$

where a and b are the zero order terms contained in states i and f respectively, and the square root term must have the correct sign of the dipole matrix element. $V(a|i)$ and $V(b|f)$ are the eigenvectors for the transformation to intermediate coupling.

For the calculation of the autoionizing rates A_a we make use of the infinite-Z, LS computations by Propin (1960, 1961, 1964). Values used are listed in Table III.

TABLE III

Autoionizing rates for large Z in LS coupling

Term	Zero-order	With configuration mixing
$1s2p^2 {}^2D$	$1{\cdot}86\ 10^{14}$	$1{\cdot}86\ 10^{14}$
$1s2p^2 {}^2S$	$1{\cdot}39\ 10^{14}$	$7{\cdot}84\ 19^{13}$
$1s2s^2 {}^2S$	$4{\cdot}1\ 10^{13}$	$1{\cdot}03\ 10^{14}$
$1s2p(^1P)2s^2P$	$1{\cdot}01\ 10^{14}$	$1{\cdot}6\ 10^{14}$
$1s2p(^3P)2s^2P$	$1{\cdot}01\ 10^{14}$	$4{\cdot}2\ 10^{13}$

In a zero-order LS scheme, the quartets do not autoionize. Nor does the $1s2p^2 {}^2P$ term. For the transformation to intermediate coupling we have a similar result to equation (16)

$$A_a(fi) = \left[\sum_{a,b} V(a|i)\, V(b|f)\sqrt{A_a(ba)}\right]^2. \qquad (17)$$

We do not know the eigenvectors $V(b|f)$ for the continuum states, but since we need only the total autoionization rate from level i, these are not required. Thus

$$A_a(i) = \sum_f A_a(fi)$$
$$= \sum_f \left[\sum_{a,b} V(a|i)\, V(b|f) \sqrt{A_a(ba)} \right]^2. \quad (18)$$

For these levels, $A_a(ba)$ is finite for only one value of b, so that the sum over b can be omitted. Then

$$A_a(i) = \sum_f [V(b|f)]^2 \left[\sum_a V(a|i) \sqrt{A_a(ba)} \right]^2$$
$$= \left[\sum_a V(a|i) \sqrt{A_a(ba)} \right]^2. \quad (19)$$

For most levels, only one term in the summation of equation (19) is finite, so that correct phases for A_a are important in only a few cases, and these can be derived from Propin's papers.

The intensities of the helium-like intercombination and forbidden lines are determined by different factors, the theory for which has been considered at length elsewhere (Gabriel & Jordan 1969b, 1972; Freeman *et al.* 1971). The relative intensities in this case depend upon electron density and are insensitive to electron temperature. If the density is less than some critical value N_e^*, the relative intensities can be derived simply if values are assumed for the ratios of excitation rates to the four $1snl$ terms. Some of these intensities are given in Table IV. The critical density is given by

$$N_e^* = \frac{0{\cdot}1 A(2^3S \rightarrow 1^1S)}{(1+F)\, C(2^3S \rightarrow 2^3P)} \quad (20)$$

where F is the excitation rate ratio $C(1^1S \rightarrow 2^3S)/C(1^1S \rightarrow 2^3P)$.

TABLE IV

Intensity ratios for the helium-like lines

Z	Ion	Intensities relative to resonance line ^1S–$^3P_1$	^1S–$^3P_2$	^1S–^3S	
6	C	0·084	0	1·02	
8	O	0·221	0·001	0·88	
10	Ne	0·25	0·008	0·84	
12	Mg	0·25	0·028	0·82	$F = 0{\cdot}45$
14	Si	0·25	0·070	0·70	$G = 1{\cdot}1$
16	S	0·25	0·13	0·64	
20	Ca	0·25	0·26	0·51	
26	Fe	0·25	0·35	0·41	
26	Fe	0·14	0·20	0·35	$F = 0{\cdot}6$, $G = 0{\cdot}7$

4. RESULTS

4.1 *Wavelengths*

To facilitate the tabulation of the results, a key letter has been assigned to each spectral line. These are listed in Table V. Tables VI and VII give the final computed

TABLE V

A list of the lines computed

Array	Multiplet	Line	Key letter
$1s^2 2p$–$1s2p^2$	$^2P^0$–^2P	$1\frac{1}{2}$–$1\frac{1}{2}$	a
		$\frac{1}{2}$–$1\frac{1}{2}$	b
		$1\frac{1}{2}$–$\frac{1}{2}$	c
		$\frac{1}{2}$–$\frac{1}{2}$	d
	$^2P^0$–^4P	$1\frac{1}{2}$–$2\frac{1}{2}$	e
		$1\frac{1}{2}$–$1\frac{1}{2}$	f
		$\frac{1}{2}$–$1\frac{1}{2}$	g
		$1\frac{1}{2}$–$\frac{1}{2}$	h
		$\frac{1}{2}$–$\frac{1}{2}$	i
	$^2P^0$–^2D	$1\frac{1}{2}$–$2\frac{1}{2}$	j
		$\frac{1}{2}$–$1\frac{1}{2}$	k
		$1\frac{1}{2}$–$1\frac{1}{2}$	l
	$^2P^0$–^2S	$1\frac{1}{2}$–$\frac{1}{2}$	m
		$\frac{1}{2}$–$\frac{1}{2}$	n
$1s^2 2p$–$1s2s^2$	$^2P^0$–^2S	$1\frac{1}{2}$–$\frac{1}{2}$	o
		$\frac{1}{2}$–$\frac{1}{2}$	p
$1s^2 2s$–$1s2p2s$	^2S–$(^1P)^2P^0$	$\frac{1}{2}$–$1\frac{1}{2}$	q
		$\frac{1}{2}$–$\frac{1}{2}$	r
	^2S–$(^3P)^2P^0$	$\frac{1}{2}$–$1\frac{1}{2}$	s
		$\frac{1}{2}$–$\frac{1}{2}$	t
	^2S–$^4P^0$	$\frac{1}{2}$–$1\frac{1}{2}$	u
		$\frac{1}{2}$–$\frac{1}{2}$	v
$1s^2$–$1s2p$	^1S–$^1P^0$	0–1	w
	^1S–$^3P^0$	0–2	x
		0–1	y
$1s^2$–$1s2s$	^1S–^3S	0–1	z

TABLE VI

Computed wavelengths in Å (see text for detailed explanation)

Multiplet	C	N	O	Ne
a–d	(41·38)	29·47	(22·05)	13·67
e–i	(41·99)	29·87	(22·33)	(13·83)
j–l	(41·55)	(29·57)	(22·11)	(13·71)
m–n	40·60	29·02	21·76	13·53
o–p	43·68	30·90	23·00	14·15
q–r	(41·33)	(29·41)	(22·02)	(13·65)
s–t	40·79	29·12	21·83	13·56
u–v	42·15	29·95	22·37	13·84
w	(40·27)	(28·79)	(21·60)	(13·45)
x–y	40·73	29·09	21·80	13·55
z	41·47	29·53	22·10	13·70

wavelengths for all the transitions in a selection of the ions studied. Values enclosed in brackets represent observed or interpolated wavelengths which have been used in adjusting the computed values. Thus all the calculated wavelengths have been adjusted on an energy scale until the resonance line wavelength (w) fits the values listed. The values for (w) have been derived from an empirical Z-expansion, chosen to fit the observations in those ions in which they are considered most

TABLE VII

Computed wavelengths in Å (cont)

Line	Mg	Si	S	Ar	Ca	Fe	Ni	Cu
a	(9·296)	6·726	5·090	3·985	3·203	1·8618	1·5974	1·4856
b	(9·292)	6·723	5·087	3·981	3·199	1·8574	1·5930	1·4812
c	(9·299)	6·730	5·094	3·989	3·207	1·8667	1·6025	1·4908
d	(9·295)	6·726	5·090	3·985	3·203	1·8624	1·5981	1·4864
e	9·382	6·782	5·128	4·012	3·223	1·8721	1·6063	1·4940
f	9·385	6·785	5·131	4·014	3·225	1·8742	1·6083	1·4958
g	9·382	6·781	5·127	4·010	3·221	1·8699	1·6038	1·4914
h	9·387	6·786	5·132	4·016	3·227	1·8762	1·6102	1·4978
i	9·383	6·783	5·129	4·012	3·223	1·8718	1·6058	1·4933
j	(9·321)	6·744	5·103	3·995	3·210	1·8657	1·6007	1·4886
k	(9·318)	6·741	5·100	3·991	3·207	1·8631	1·5982	1·4862
l	(9·321)	6·744	5·104	3·995	3·211	1·8674	1·6026	1·4906
m	(9·221)	6·682	5·062	3·966	3·189	1·8562	1·5930	1·4816
n	(9·218)	6·678	5·058	3·962	3·185	1·8519	1·5886	1·4773
o	9·569	6·898	5·205	4·065	3·262	1·8895	1·6201	1·5063
p	9·566	6·894	5·201	4·061	3·257	1·8850	1·6156	1·5018
q	(9·283)	6·718	5·085	3·981	3·200	1·8604	1·5963	1·4846
r	(9·286)	6·720	5·087	3·983	3·202	1·8635	1·5996	1·4822
s	(9·235)	6·689	5·066	3·968	3·191	1·8564	1·5931	1·4818
t	(9·236)	6·690	5·067	3·969	3·192	1·8570	1·5936	1·4880
u	9·390	6·786	5·131	4·014	3·224	1·8730	1·6070	1·4945
v	9·392	6·788	5·133	4·015	3·226	1·8743	1·6083	1·4958
w	(9·168)	(6·647)	(5·038)	(3·948)	(3·176)	(1·8500)	(1·5880)	(1·4771)
x	9·228	6·685	5·063	3·965	3·189	1·8551	1·5919	1·4807
y	9·231	6·688	5·066	3·969	3·192	1·8591	1·5961	1·4849
z	9·313	6·739	5·101	3·993	3·210	1·8677	1·6031	1·4913

reliable. Wavelengths for the forbidden line (*z*) have been derived from the results of Vainstein and Safronova, as indicated above. Wavelengths for the lines (o) and (p) may be less accurate than the others. There are as yet no positive identifications of this multiplet in observed spectra.

Fig. 1 shows a plot of the energy difference between each transition and the LS coupled resonance line. In this way it is possible to see the effects of the spin-orbit interaction on all the transitions, including the resonance line. This plot is in effect an extension to higher Z of the one given by Gabriel & Jordan (1969a). It shows clearly the dangers of straight line extrapolation of the earlier plot to higher Z, as has been attempted by Neupert (1971), Walker & Rugge (1971) and Doschek *et al.* (1971a). Such an extrapolation can easily lead to errors in identifying lines, as has in fact occurred. Not all of the lines are shown on Fig. 1, but in general only those whose intensity by dielectronic recombination are predicted to exceed 0·5 per cent of the total satellite intensity for that ion.

4.2 *Intensities*

The intensities of the satellites depend primarily on the computed values for A_r and A_a. These have been listed for four ions in Table VIII. The change of A_a with Z is due entirely to the trend towards intermediate coupling, whereas the values for A_r are influenced in addition by an overall Z^4 dependence.

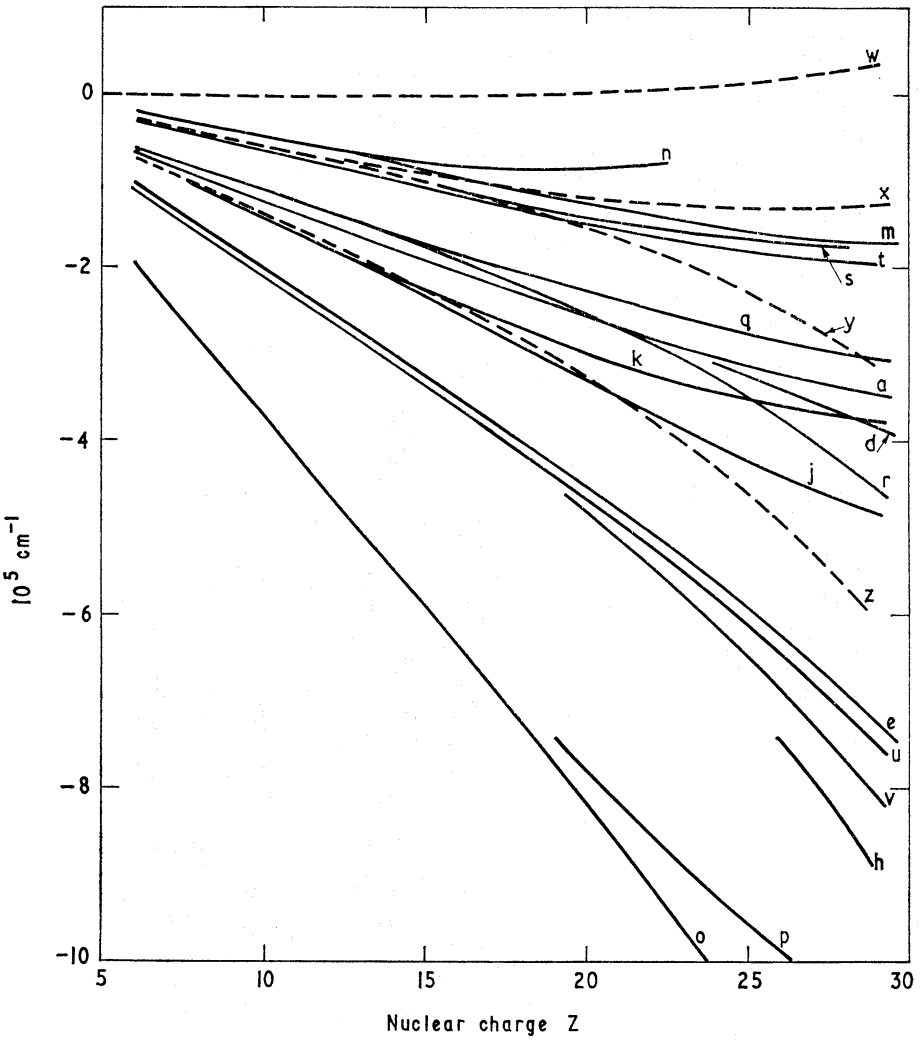

FIG. 1. *Computed energies of the transitions, plotted as displacements from the computed LS coupling energy of the helium-like resonance line.*

Tabulation of the intensities is aided by defining a characteristic temperature T_m for each ion. For convenience this has been chosen as the temperature at which the helium-like ion resonance line has its maximum emission in an isothermal steady state plasma. It occurs at the maximum of the function $g(T)$ (Pottasch 1963), given by

$$g(T) = \frac{\exp(-E_0/kT)}{T^{1/2}} \frac{N_{He}}{N(E)}. \quad (21)$$

The ionization equilibrium $N_{He}/N(E)$ has been taken from the calculations of Jordan (1969, 1970). T_m can be fitted empirically by the expression

$$T_m = 8230(Z-0{\cdot}6)^{2{\cdot}71}. \quad (22)$$

Values of T_m from equation (22) have been listed in Table IX, together with the characteristic densities N_e'', N_e' and N_e^* given by equations (6), (13) and (20) respectively.

TABLE VIII

Computed transition probabilities in units of $10^{13}\ s^{-1}$

	O		Si		Ca		Fe	
Line	A_r	A_a	A_r	A_a	A_r	A_a	A_r	A_a
a	0·411	0·016	5·09	0·235	23·8	1·18	70·6	2·69
b	0·075	0·016	0·702	0·235	1·85	1·18	2·54	2·69
c	0·160	—	1·80	0·016	6·88	0·136	16·0	0·394
d	0·326	—	4·03	0·016	19·5	0·136	60·8	0·394
e	—	0·002	0·007	0·065	0·309	0·654	4·27	2·98
f	—	—	0·001	0·010	0·041	0·101	0·575	0·505
g	—	—	0·003	0·010	0·109	0·101	1·62	0·505
h	—	—	0·002	0·003	0·070	0·023	0·630	0·055
i	—	—	—	0·003	—	0·023	0·024	0·055
j	0·161	18·6	1·92	18·5	8·56	17·9	22·6	15·6
k	0·140	18·6	1·88	18·4	9·93	17·3	31·9	15·4
l	0·021	18·6	0·101	18·4	—	17·3	1·06	15·4
m	0·101	7·82	1·33	7·99	7·42	7·90	27·0	7·53
n	0·048	7·82	0·442	7·99	0·989	7·90	0·635	7·53
o	0·011	10·2	0·132	9·97	0·561	9·92	1·52	10·0
p	0·006	10·2	0·074	9·97	0·396	9·92	1·62	10·0
q	0·296	16·0	3·57	15·7	16·9	14·5	52·0	12·4
r	0·293	16·2	3·31	17·4	13·0	19·1	29·8	20·1
s	0·031	4·23	0·335	4·47	0·926	5·63	0·712	7·73
t	0·034	3·99	0·601	2·85	4·92	1·10	24·0	0·065
u	—	—	0·003	0·003	0·121	0·026	1·56	0·101
v	—	—	0·001	0·001	0·040	0·009	0·448	0·034

TABLE IX

Characteristic temperatures and approximate values of critical densities

		T_m	N_e''	N_e'	N_e^*	N_{Li}/N_{He}
Z	Ion	(10^6 °K)	(cm^{-3})	(cm^{-3})	(cm^{-3})	at T_m
6	C	0·79	2.10^{12}	2.10^{15}	6.10^{7}	0·001
7	N	1·26	1.10^{13}	6.10^{15}	7.10^{8}	0·002
8	O	1·87	5.10^{13}	1.10^{16}	4.10^{9}	0·004
10	Ne	3·57	5.10^{14}	5.10^{16}	7.10^{10}	0·007
12	Mg	6·02	3.10^{15}	1.10^{17}	7.10^{11}	0·012
14	Si	9·33	2.10^{16}	3.10^{17}	4.10^{12}	0·018
16	S	13·6	1.10^{17}	5.10^{17}	2.10^{13}	0·025
18	Ar	18·9	2.10^{17}	1.10^{18}	7.10^{13}	0·034
20	Ca	25·4	6.10^{17}	2.10^{18}	2.10^{14}	0·043
26	Fe	52·8	7.10^{18}	5.10^{18}	5.10^{15}	0·079
28	Ni	64·8	1.10^{19}	7.10^{18}	1.10^{16}	0·094
29	Cu	71·4	2.10^{19}	8.10^{18}	2.10^{16}	0·101

Equation (7) showed how the relative intensity of the satellite I_s/I could be separated into electron temperature and satellite dependent terms. For the purposes of tabulating the results we rewrite equation (7) as

$$\left(\frac{I_s}{I}\right)_T = \frac{\dfrac{1}{(1+\alpha(T))}F_1(T)}{\dfrac{1}{(1+\alpha(T_m))}F_1(T_m)} \times \left(\frac{I_s}{I}\right)_{T_m}. \qquad (23)$$

TABLE X

Values of the satellite/resonance line intensity ratios for dielectronic recombination and inner-shell excitation, computed at $T = T_m$ *and* $T_z = T_m$ *respectively. These must be multiplied by the temperature factors in Fig. 2, and for inner-shell excitation by the factor* β

	O		Si		Ca		Fe	
Line	I_s/I	I_s'/I	I_s/I	I_s'/I	I_s/I	I_s'/I	I_s/I	I_s'/I
a	0·0004	0·0008	0·0033	0·0049	0·0119	0·0124	0·0217	0·0231
b	0·0001	0·0001	0·0005	0·0007	0·0009	0·0010	0·0008	0·0008
c	—	0·0002	—	0·0009	0·0002	0·0018	0·0004	0·0026
d	—	0·0003	0·0001	0·0020	0·0006	0·0051	0·0013	0·0098
e	—	—	0·0002	0·0002	0·0036	0·0017	0·0228	0·0055
f	—	—	—	0·0001	0·0002	0·0006	0·0009	0·0013
g	—	—	—	0·0003	0·0005	0·0015	0·0026	0·0037
h	—	—	—	0·0003	0·0001	0·0013	0·0002	0·0028
i	—	—	—	—	—	—	—	0·0001
j	0·0070	—	0·0441	0·0007	0·0991	0·0057	0·1200	0·0191
k	0·0041	—	0·0286	0·0004	0·0719	0·0043	0·0880	0·0142
l	0·0006	—	0·0015	—	—	—	0·0029	0·0005
m	0·0015	—	0·0092	0·0001	0·0205	0·0010	0·0250	0·0035
n	0·0007	—	0·0031	—	0·0027	0·0001	0·0006	0·0001
o	0·0002	—	0·0011	—	0·0029	—	0·0050	0·0002
p	0·0001	—	0·0006	—	0·0021	—	0·0053	0·0002
q	0·0085	—	0·0491	0·0019	0·0890	0·0135	0·0865	0·0360
r	0·0042	—	0·0234	0·0008	0·0440	0·0051	0·0520	0·0133
s	0·0009	—	0·0053	0·0002	0·0091	0·0012	0·0056	0·0013
t	0·0005	—	0·0042	0·0003	0·0051	0·0034	0·0003	0·0074
u	—	—	—	0·0008	0·0002	0·0034	0·0008	0·0070
v	—	—	—	0·0004	—	0·0017	0·0001	0·0035
Total	0·0287		0·1744		0·3647		0·4431	

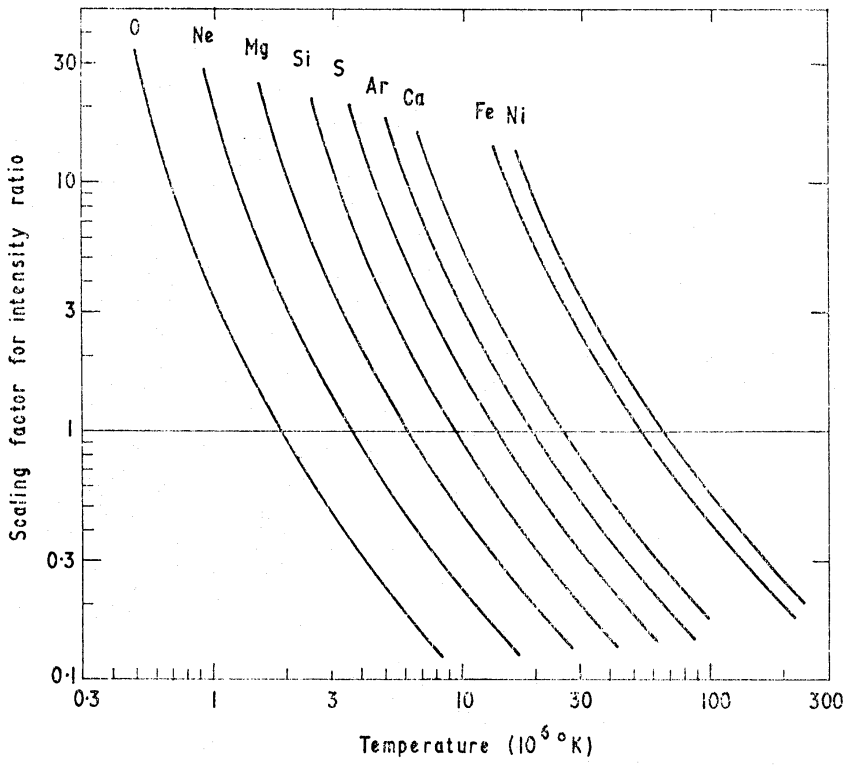

FIG. 2. *Multiplying factors for intensity ratios, at temperatures other than* T_m.

The second factor, i.e. the ratio I_s/I computed at the characteristic temperature T_m, is given in Table X, while the first factor, the multiplying factor for other temperatures, is plotted graphically in Fig. 2. The intensity factors I_s/I in Table X have been computed for low densities using the value $\bar{f} = 0{\cdot}55$. For densities greater than N_e'' (as given in Table IX) the ratios must be multiplied by 0·55/0·75 or 0·73 to allow for $1s2s\,^1S \rightarrow 1s2p\,^1P$ excitation. Fig. 3 shows how these ratios

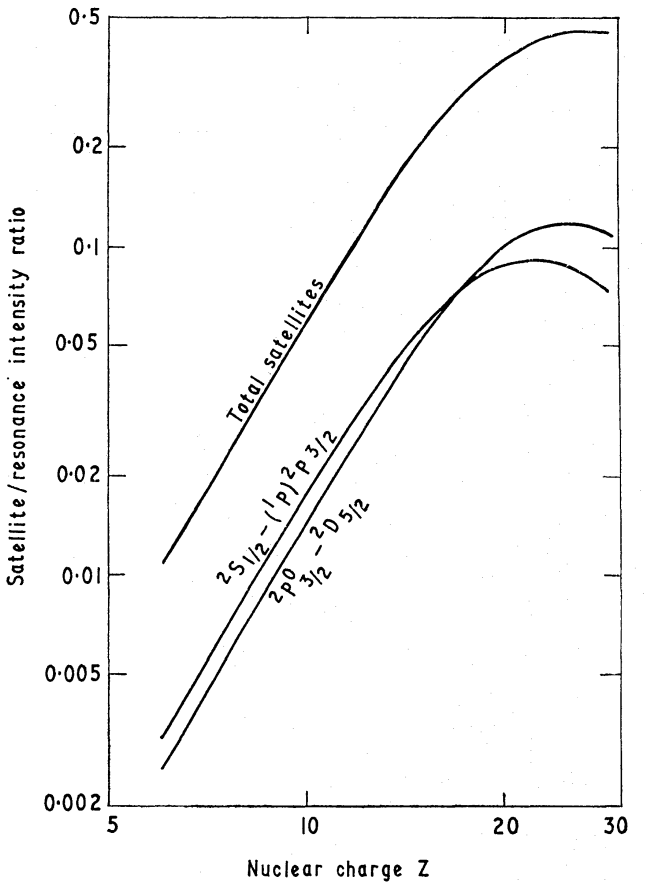

FIG. 3. *Graph showing the variation with Z of the satellite/resonance line intensity ratios by dielectronic recombination, at the characteristic temperature* T_m.

vary as a function of Z, showing the total satellites as well as the two stronger components. The straight line portion representing the limiting trend at low Z curves over as A_r becomes comparable with A_a.

The intensity ratio by inner-shell excitation can be written similarly

$$\left(\frac{I_s'}{I}\right)_{T_z} = \frac{\dfrac{1}{(1+\alpha(T))}\,F_1'(T_z)}{\dfrac{1}{(1+\alpha(T_m))}\,F_1'(T_m)} \times \left(\frac{I_s'}{I}\right)_{T_m}. \qquad (24)$$

$F_1'(T_z)$ can be computed from the ionization equilibrium calculations of Jordan (1969, 1970). However, it can readily be shown that, to within close limits, the temperature factor in equation (24) is the same function of T_z as the factor in equation (23) is of T. It is therefore permissible to use the curves of Fig. 2 for both. The error introduced by assuming that α in equation (24) is a function of T_z

instead of T can be safely neglected since α does not normally exceed $\sim 0{\cdot}1$. The ratios I_s'/I are listed for $T_z = T_m$ in Table X, taking $\beta = 1$, and $\bar{f} = 0{\cdot}55$. These must be multiplied by β as given in Section 2.2 depending on whether N_e is greater or smaller than N_e', and also by 0·73 as above if N_e is greater than N_e''. Note that the contribution to the satellite intensity from inner-shell excitation increases at higher Z, relative to the dielectronic contribution. This is due to the increase with Z of N_{Li}/N_{He} at T_m as shown in Table IX.

4.3 *Errors*

There is no means of estimating theoretically the probable errors in the computed wavelengths. However, comparison with observations shows a remarkable agreement as will be seen later.

The intensity ratios depend upon the values of A_r, A_a and $\bar{f}'$. Errors can always increase where large cancellations occur through the transition to intermediate coupling. Thus, satellites which are weak at high Z but not at low Z will have unreliable intensities. In general the stronger satellites will be more reliable. Values of A_r will be very reliable—probably better than 10 per cent. Thus the dielectronic contribution at low Z will be limited in accuracy mainly by $\bar{f}$ for the resonance line to about ± 25 per cent in intensity or 10–15 per cent in T. Values of A_a will be less reliable, perhaps only 50 per cent. These have little effect at low Z but will by iron be limiting the intensity accuracy by a further ± 25 per cent leading to an overall accuracy in T of ~ 25 per cent.

Inner-shell excitation will be limited to a factor ~ 2 by uncertainties in $\bar{f}'$, or the effective excitation rate. For the stronger satellites, however, the inner-shell contribution is less than 25 per cent of the total if $T_z = T$, even in iron. It only becomes dominant when $T_z < T$, i.e. in an ionizing plasma. In this region the temperature dependence becomes steeper, so that a factor of 2 in I_s'/I leads to only a factor of ~ 30 per cent in T_z.

4.4 *Comparison with other calculations*

Calculations of the transition energies for these satellites have been made by Cowan (1968, private communication) using a modified Hartree–Fock–Slater technique. These *ab initio* calculations have not benefited from the adjustments and cancellation of errors of the present calculation. An accuracy of 0·002 Å in iron in Cowan's calculations is not quite sufficient to identify observed spectra. Cowan also computes A_r and these agree well with the present values.

Vainstein & Safronova (1971b) have calculated the energies, A_r and A_a for all the satellites. Their wavelengths, calculated using a Z-expansion method, agree well with the present values. However, in the preliminary preprint received, their values for A_r and A_a differ appreciably from the present calculations as well as from the A_r values of Cowan. In view of the agreement between Cowan and the present calculations, it appears that Vainstein and Safronova are in error in their transition probability calculations.

5. COMPARISON WITH OBSERVATIONS

5.1 *Solar spectra*

Only a few observations are available of sufficient resolution to compare in detail with these calculations. At lower Z a very fine spectrum has recently been

reported by Parkinson (1972) in magnesium. It has been used as a standard in order to adjust some of the computed wavelengths in the present work, as indicated in Section 3.1. A comparison of the intensities with the present calculations has been carried out in Parkinson's paper. At this low value of Z, inner-shell excitation is negligible, so that no values of T_z can be deduced. The value for T which gives the best fit is 4.10^6 °K.

A spectrum of silicon recorded from an active region by Walker & Rugge (1971) is shown in Fig. 4, together with the presently computed spectrum. The strong

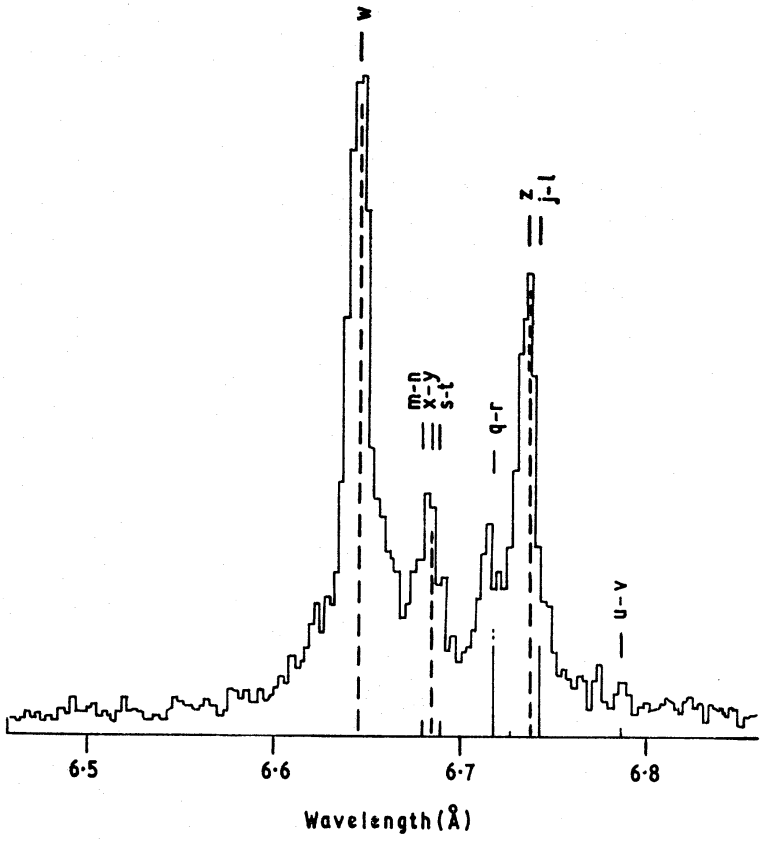

FIG. 4. *Solar flare spectrum of silicon (Walker & Rugge 1971). The vertical lines represent the computed spectrum. Dashed lines are due to the helium-like ion, solid lines are dielectronic recombination satellites and dotted lines are inner-shell excited satellites. Key letters refer to the transitions in Table V.* $T = 7{\cdot}5.10^6$ °K, $T_z = 3.10^6$ °K.

dielectronic satellite $(q-r)$ is used to determine the electron temperature T as $7{\cdot}5.10^{6}$K. If the feature identified as $(u–v)$ is significant its intensity can only be produced by an enhanced inner-shell excitation. This then gives $T_z = 3.10^6$ °K and implies an ionizing plasma, which is perhaps a little surprising in a non-flaring active region.

For calcium there are no good solar spectra, the best available being that reported by Doschek *et al.* (1971b). This has been reproduced in Fig. 5, where the crosses are the observed points and the smooth curve is a computor best-fit to an assumed 5-line spectrum. Also shown is the computed spectrum. In this case the quality is not sufficient to determine the inner-shell excitation contribution, and it has been assumed that $T_z = T$. This then gives a value for T of 17.10^6 °K.

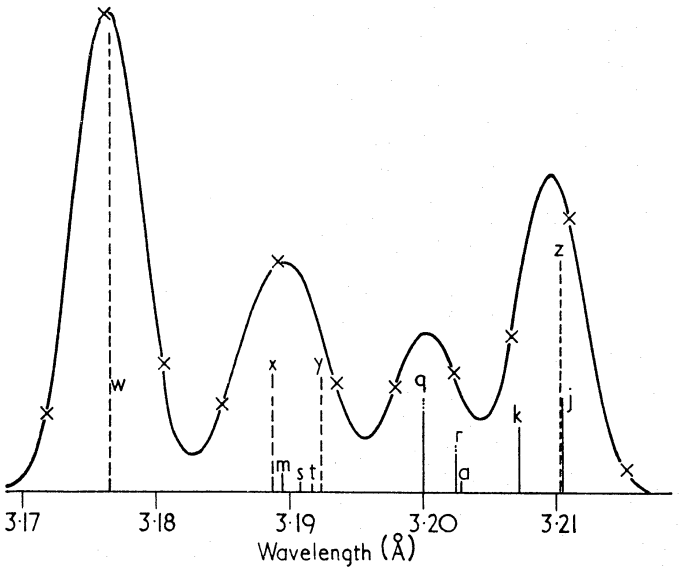

FIG. 5. *Solar flare spectrum of calcium reported by Doschek* et al. (1971*b*). *The computed spectrum is for* $T = 17.10^6\,°K$.

A very fine iron spectrum has been recorded from a solar flare by the Intercosmos-4 orbiting vehicle. This has been reported by Grineva *et al.* (1971), who also assigned identifications based on the calculations of Vainstein and Safronova. The spectrum is shown in Fig. 6, together with a computed spectrum from the present work. First note the wavelength agreement of 0·0001 Å for the satellite calculations for the $1s^2 2p - 1s2p^2$ array and 0·0003 Å for the $1s^2 2s - 1s2s2p$ array. This is rather better than Vainstein and Safronova, although it is fair to point out

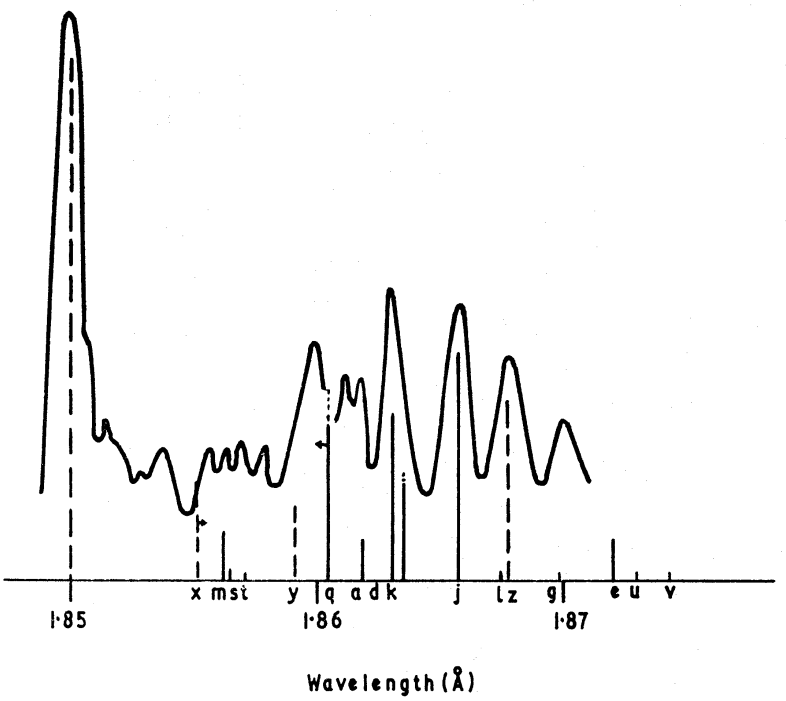

FIG. 6. *Solar flare spectrum of iron by Grineva* et al. (1971). *The computed spectrum is for* $T = 26.10^6\,°K$ *and* $T_z = 50.10^6\,°K$. *The un-marked line to the right of that designated* k *should be designated as* r

that theirs is a fully *ab initio* calculation, whereas the present values have been adjusted to fit lower Z observations. In fitting the intensities, the pure dielectronic satellite (j) gives a clear determination of the electron temperature T of 26.10^6°K, in good agreement with the thermal Doppler ion temperature measured by Grineva *et al.* of 30.10^6°K. Since the spectrum does not extend out as far as the quartet levels, only the satellite (q) is available to determine the inner-shell contribution. A best fit gives $T_z = 50.10^6$°K, although not with a high accuracy. This implies a recombining plasma, which is not surprising for a solar flare. It should be mentioned that in order to fit the intensities of the helium-like Fe XXV lines it is necessary to adopt the values for the parameters F and G given in the final row of Table IV, in place of the values adopted for the other ions.

The identifications implied by this comparison are in agreement with those assigned in the paper by Grineva *et al.* The feature at 1·870 Å was attributed by Grineva *et al.* to a $1s-2p$ transition in Be-like Fe XXIII. It is assumed that the features close to the resonance line are due to satellites in which the third electron is in an $n = 3$ shell.

5.2 *Laboratory plasmas*

Laboratory spectra of helium-like ions can at present be produced at high Z only in devices which operate on an impulsive pinch effect. These include the so-called ' plasma focus ' (Peacock, Hobby & Morgan 1971) and some low inductance vacuum sparks (Cohen *et al.* 1968; Lie & Elton 1971; Schwob & Fraenkel 1972). These devices have very short time scales, $\sim 10^{-7}$ s. A general feature of the spectra is a series of broad peaks on the long wavelength side of the helium-like resonance line extending as far as the K_α X-ray line of the neutral ion. By comparison with the Hartree–Fock calculations of House (1969) these have been attributed to $1s$–$2p$ transitions in successively lower ion stages. An impressive example, shown in Fig. 7, is the spectrum of a low-inductance iron spark by Schwob & Fraenkel (1972).

In the present paper, two alternative mechanisms have been considered for the production of the 3-electron satellites. As one goes to lower ion stages, the number of possible mechanisms increases rapidly and the situation becomes very complex. What is clear, however, is that the production of these states requires similar or more extreme conditions to the inner-shell excitation of 3-electron ions; i.e. the presence of low ion stages combined with a high electron temperature, or a rapidly ionizing plasma. Solar spectra on the other hand do not show this extended system of ion stages, and this can now be understood since they do not have these extreme transient ionizing conditions.

Further support for this interpretation can be found by a closer study of the lithium-like ion satellites. Fig. 8 shows the relevant portion of the above spectrum expanded. Resolution is somewhat limited by Doppler broadening due to the very high ion motions in the plasma. This laboratory plasma is believed to have a density well above the three critical values given in Table IX, and the predicted intensity has been derived accordingly. The best fit with the computed intensities is given by ignoring the dielectronic recombination mechanism and assuming that the total contribution comes from direct inner-shell excitation. It is not possible therefore to obtain a value for the electron temperature, but the value of T_z derived is 9.10^6°K. This is consistent with a rapid ionization and with estimates of electron

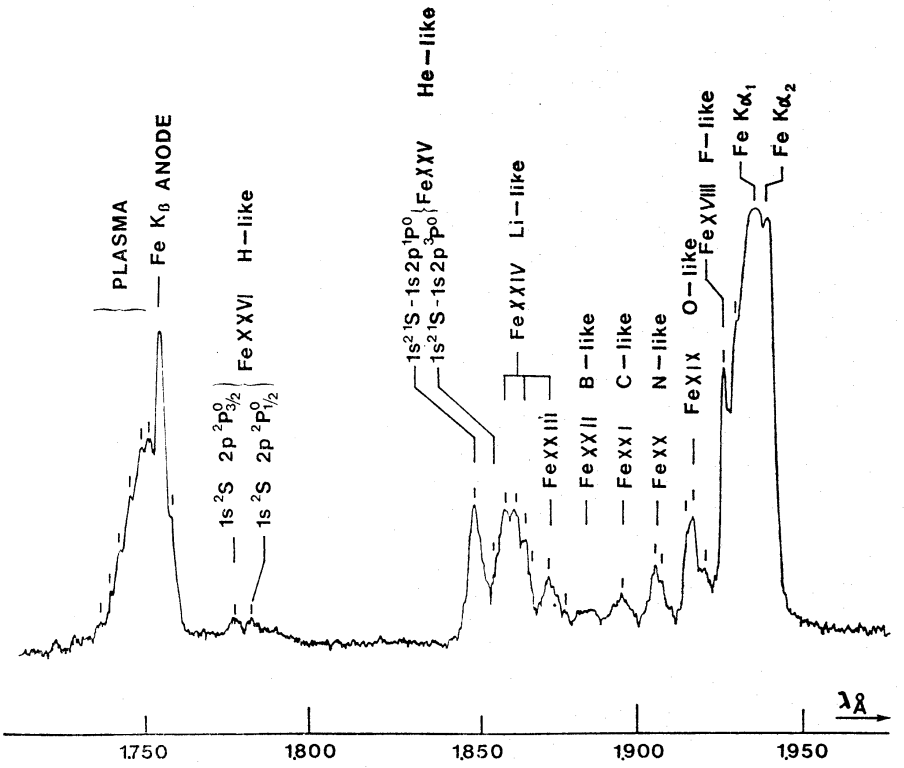

FIG. 7. *Spectrum of a low inductance spark by Schwob & Fraenkel* (1972). *This shows inner-shell* 1s–2p *transitions in a wide range of iron ions.*

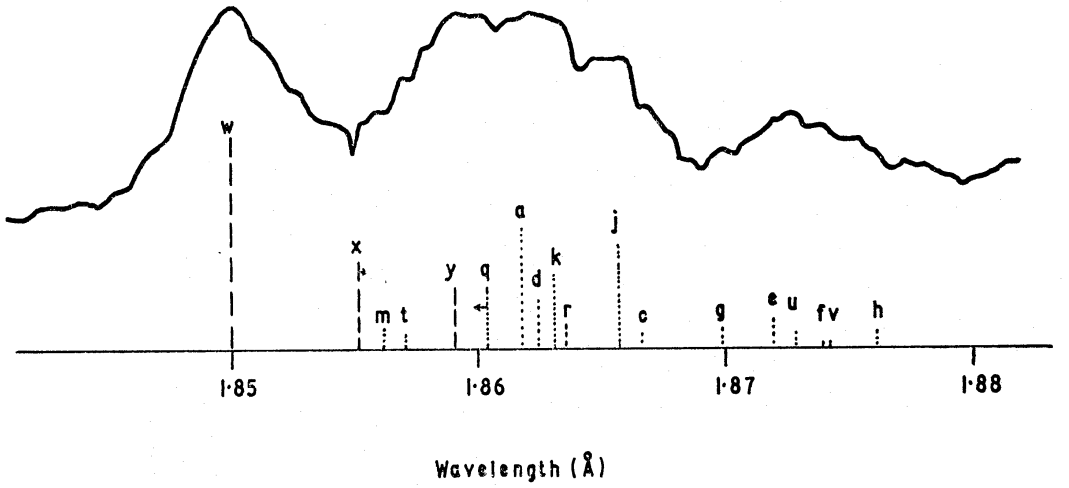

FIG. 8. *A portion of the spectrum of Fig. 7 expanded and compared with a pure inner-shell excitation spectrum computed from the present theory for* $T_z = 9.10^6\,°K$.

temperature in these sources given by their authors' of up to $300.10^6\,°K$. It appears therefore that the laboratory production of spectra similar to that in Fig. 6 will have to await the development of a new type of source.

6. CONCLUSIONS

Calculations have been carried out in order to predict the wavelengths and intensities of the satellite lines to the helium-like ion resonance line for highly

charged ions. For the wavelengths, the reliability has been greatly improved by working entirely with the computed energy difference between the satellites and the resonance line, as well as by adjusting the computation to fit reliable observations at low Z. For the intensities, contributions have been derived for the two principal mechanisms; dielectronic recombination and inner-shell excitation. In fitting these to an observed spectrum, it is possible in principle to determine both the electron temperature and the relative distribution of ion stages. Taken together, these two factors determine whether the plasma is ionizing, steady state or recombining. Although the present calculations have been completed for all ions from carbon to copper, only a selection of this data has been reproduced in the present paper. The author will be glad to supply further data if requested.

These results have been applied to the best available solar and laboratory spectra. The electron temperatures obtained for solar plasmas are always below T_m, the characteristic temperature at which the resonance line has its maximum emission. Values obtained range from 80 per cent of T_m for active region spectra, to 50 per cent of T_m for iron spectra from solar flares. This can be readily understood in terms of an emission measure, $\int N_e^2\, dv$, which decreases with the electron temperature. Analysis of the transient state indicates ionization in the active regions and recombination in the solar flares, in the particular examples studied.

Laboratory low-inductance spark plasmas appear to show evidence of extreme transient ionization, and are thus somewhat different from the solar spectra. The 3-electron satellites are produced mainly by inner-shell excitation, and there are also strong features associated with $1s$–$2p$ transitions in successively lower ion stages.

The group of lines in the region of the helium-like ion resonance line have been shown to have important diagnostic possibilities. Very few of the solar spectra so far obtained are of sufficient quality to exploit this fully. The importance of obtaining further solar flare spectra, particularly in iron, is strongly emphasized by the present analysis. The possibility of important Fe XXV emission has been widely discussed also in connection with cosmic X-ray sources, in particular Sco–X1. If this is so, it will certainly be accompanied by a prominent system of satellite lines. Studies of the escape of such radiation from an optically thick atmosphere should take account of these, and in this the present calculations may be useful. Lines escaping more readily on account of their low self-absorption will include not only the helium-like forbidden line $1s^2\,{}^1S$–$1s2s\,{}^3S$ but also satellites from the array $1s^2 2p$–$1s2p^2$, which end on an excited term.

ACKNOWLEDGMENTS

I would like to thank several colleagues for advice on important points regarding these calculations, and in particular Dr N. Spector, Dr I. P. Grant, Professor L. A. Vainstein, Professor A. Dalgarno and Dr A. Ermolaev. I am grateful to Professor Mandelstam for permission to reproduce the Intercosmos-4 spectrum in Fig. 6. I would also like to thank Robert Smith for assistance with some of the earlier computations.

Astrophysics Research Unit, Culham Laboratory, Abingdon, Berkshire

REFERENCES

Burgess, A., 1965. *Astrophys. J.*, **141**, 1588.
Cohen, L., Feldman, U., Swartz, M. & Underwood, J. H., 1968. *J. opt. Soc. Am.*, **58**, 843.
Doschek, G. A., Meekins, J. F., Kreplin, R. W., Chubb, T. A. & Friedman, H., 1971a. *Astrophys. J.*, **170**, 573.
Doschek, G. A., Meekins, J. F., Kreplin, R. W., Chubb, T. A. & Friedman, H., 1971b. *Astrophys. J.*, **164**, 165.
Edlén, B. & Tyrén, F., 1939. *Nature*, **143**, 940.
Freeman, F. F., Gabriel, A. H., Jones, B. B. & Jordan, C., 1971. *Phil. Trans. R. Soc. Lond. A.*, **270**, 127.
Froese, C., 1969. *Computer Phys. Commun.*, **1**, 151.
Gabriel, A. H. & Jordan, C., 1969a. *Nature*, **221**, 947.
Gabriel, A. H. & Jordan, C., 1969b. *Mon. Not. R. astr. Soc.*, **145**, 241.
Gabriel, A. H. & Jordan, C., 1972. Chapter in *Case Studies in Atomic Collision Physics—II*, eds McDaniel and McDowell, North-Holland.
Gabriel, A. H., Jordan, C. & Paget, T. M., 1969. *Proc. 6th Int. Conf. on Physics of Electronic and Atomic Collisions* (MIT Press, Mass., USA), p. 558.
Gabriel, A. H. & Paget, T. M., 1972. *J. Phys. B.*, **5**, 673 (Paper I).
Grineva, Yu. I., Karev, V. I., Korneev, V. V., Krutov, V. V., Mandelstam, S. L., Vainstein, L. A., Vasiljev, B. N. & Zitnik, I. A., 1971. Paper presented at COSPAR, Seattle; to be published in *Kosmicheskie Issledovaniya*, USSR.
House, L. L., 1969. *Astrophys. J. Suppl.*, **18**, 21.
Jordan, C., 1969. *Mon. Not. R. astr. Soc.*, **142**, 501.
Jordan, C., 1970. *Mon. Not. R. astr. Soc.*, **148**, 17.
Lie, T. N. & Elton, R. C., 1971. *Phys. Rev. A.*, **3**, 865.
Neupert, W. M., 1971. *Sol. Phys.*, **18**, 474.
Parkinson, J. H., 1972. *Nature* (*Phys. Sci.*), **236**, 68.
Peacock, N. J., Hobby, M. G. & Morgan, P. D., 1971. *Plasma Physics and Controlled Fusion*, Vol. 1, p. 537 (IAEA, Vienna).
Pottasch, S. R., 1963. *Astrophys. J.*, **137**, 945.
Propin, R. Kh., 1960. *Optics Spectrosc.*, **8**, 158.
Propin, R. Kh., 1961. *Optics Spectrosc.*, **10**, 155.
Propin, R. Kh., 1964. *Optics Spectrosc.*, **17**, 332.
Schwob, J. L. & Fraenkel, B. S., 1972. *Space Sci. Rev.*, to be published.
Shore, B. W., 1969. *Astrophys. J.*, **158**, 1205.
Vainstein, L. A. & Safronova, U. I., 1971a. *Sov. Astr. AJ*, **15**, 175.
Vainstein, L. A. & Safronova, U. I., 1971b. Private communication, to be published in *Short Communications in Physics* (Lebedev Institute).
Van Regemorter, H., 1962. *Astrophys. J.*, **136**, 906.
Walker, A. B. C. & Rugge, H. R., 1971. *Astrophys. J.*, **164**, 181.